A hybrid radiation detector for simultaneous spatial and temporal dosimetry

C. Poole[1] , J.V. Trapp[1*], J. Kenny[2] ,T. Kairn[2] , K. Williams[3], M. Taylor[3], R. Franich[3], C.M. Langton[1]

1. *Physics, Faculty of Science and Technology, Queensland University of Technology, GPO Box 2434, Brisbane Qld 4001, Australia*

2. *Premion, The Wesley Medical Centre, Suite 1 40 Chasely Street, Auchenflower Queensland 4066, Australia*

3. *School of Applied Sciences, RMIT University, GPO Box 2476, Melbourne 3001, Australia*

*Corresponding Author: Email: j.trapp@qut.edu.au, Phone +61 7 31381386, Fax +61 7 1389079

Abstract

In this feasibility study an organic plastic scintillator is calibrated against ionisation chamber measurements and then embedded in a polymer gel dosimeter to obtain a quasi-4D experimental measurement of a radiation field. This hybrid dosimeter was irradiated with a linear accelerator, with temporal measurements of the dose rate being acquired by the scintillator and spatial measurements acquired with the gel dosimeter. The detectors employed in this work are radiologically equivalent; and we show that neither detector perturbs the intensity of the radiation field of the other. By employing these detectors in concert, spatial and temporal variations in the radiation intensity can now be detected and gel dosimeters can be calibrated for absolute dose from a single irradiation.

Introduction

With the increasing clinical use of radiotherapy techniques that rely on the accurate spatial and temporal variation of dose delivery [1-5] there is a growing need for the ability to fully characterise a radiation field, in four dimensions.

Contemporary radiation detectors are capable of measuring radiation dose in one, two, or three dimensions. For example, dosimeters utilizing Fricke solution [6-8] , polymers [9-16] and dyed plastics [17, 18] have been successful in measuring radiation dose in three dimensions but not temporally. Electronic portal imaging devices (EPIDs) based on fluoroscopic [19, 20] or solid-state radiation detection [21], as well as planar detector arrays [22] are capable of measuring radiation fields in two spatial dimensions. Recently, diode-array based detectors have been developed which are designed to provide three-dimensional evaluations of delivered dose [23, 24]. All of these dosimeter-array-based systems, including EPIDs, are capable of providing information regarding the variation of the radiation beam with time; however all of these systems (including those specifically designed to measure in three-dimensions) use back-projection techniques, rather than explicit three-dimensional measurement, to provide three-dimensional dosimetric information [23-25].

To date there has been no dosimetry system for measuring radiation dose in three spatial dimensions as well as time. An intermediate solution would be to combine two different radiation detection systems which are radiologically similar, to measure different characteristics of the same radiation field. This technique requires that each detector used must not perturb the measurement of the other. In this feasibility study we combine an organic plastic scintillator for temporal measurements with a polymer gel dosimeter for 3D spatial measurements to produce a quasi four-dimensional hybrid radiation dosimetry system.

Methods and Materials

The dosimetry was achieved by combing a BC-428 organic plastic scintillator rod of 5mm diameter and 6mm length (Saint Gobain, Paris) for temporal measurements, with a PAGAT polymer gel dosimeter [16] for spatial

3

measurement. The densities of the PAGAT [16] gel dosimeter and organic plastic scintillators are closely matched at 1.026 ± 0.02 [16] and 1.032 g/cm^3 [26] respectively and a previous Monte Carlo study has shown that these two detectors are dosimetrically similar [27]. The scintillator was optically coupled to a S2386-44K photodiode (Hammamatsu, Japan) and electronic circuitry similar to that described elsewhere [28]. Both the scintillator and the gel dosimeter were encased in an acrylic cylinder container of 13 cm outer diameter and 15 cm length, with walls of 5 mm thickness.

Dose and dose rate responses of the scintillator were calibrated with a 6 MV photon beam produced using a Clinac 6EX (Varian Inc., CA, USA) clinical linear accelerator. The scintillator was positioned on-axis within a Virtual Water (Standard Imaging, WI, USA) phantom at 100 cm SSD, a depth of 4.5 cm and irradiated with a 3×3 cm field. The scintillator was then irradiated at various dose rates as shown in figure 2 by varying the monitor units per minute and compared to calibrated ionization chamber data. The signal was taken as the mean output frequency of the detector electronics [28] sampled at regular intervals and the uncertainty was the standard deviation of the measurements. An angle of 90 degrees between the axis of the beam and the fibre optic coupling was maintained. After calibration, the scintillator was secured in place at the central axis of the cylindrical acrylic container at a location 3cm from the end wall, and such that the optical coupling fibre penetrated the outer wall of the container at the same height as shown in figure 1.

The gel dosimeter was manufactured according to the composition published by Venning et al [16], however the concentration of Tetrakis Hydroxy Phosphonium Chloride was increased to 8 mM for improved stability [29] as shown at Table 1. Before cooling and setting, the gel dosimeter was poured into the acrylic container containing the scintillator so that the scintillator was completely immersed as shown in Figure 1. The container was then placed in a refrigerator and stored at 4°C for 24 hours to allow the gel dosimeter to set, after which it was pre-scanned in an MGS Research IQScan optical CT scanner (MGS Research, (Madison, CT, USA).

The container enclosing the scintillator and gel dosimeter was then irradiated with two 3 cm $\times$ 3 cm 6 MV X-ray beams from the same linear accelerator that was used for calibration of the scintillator, with 2cm of solid water placed on top of the container. This ensured that any effects of Cerenkov radiation equally applied to both the calibration and the irradiation. Both radiation beams were delivered to the same location and orientation (centrally

along the cylindrical axis); however the radiation output of the linear accelerator was varied so that they produced 2.50 ± 0.03 Gy/minute for 60 seconds and 5.00 ± 0.05 Gy/minute for 30 seconds at the scintillator respectively, giving a total dose of 5 Gy. Because the scintillator and sheath were directly in conact with the gel dosimeter, electronic equilibrium was not disturbed at the boundary as shown previously[27]. The dose rates of the beams were measured with the scintillator at the time of delivery. It has been shown [30, 31] that dose rate effects within PAGAT gel dosimeters are negligible for the range of dose rates and total dose delivered in this experiment.

After 24 hours the container enclosing the gel dosimeter and the scintillator was scanned in a MGS Research IQScan optical CT scanner (Madison, CT, USA). The pre-scan data was then subtracted prior to image reconstruction to remove any optical inhomogeneities in the gel. Data processing was performed using Matlab (The Mathworks, USA).

Results

Figure 2 shows the calibration data for the scintillator and shows an increasing response of output with respect to increasing dose rate. The data provides an R^2 value of 0.998 and p value of 6×10^{-7} for a 95% confidence level. From this data we make the assumption of a linear dose rate response of the total scintillator measurement for those dose rates employed in this work. Possible contributions from Cerenkov radiation to the signal are discussed in the following section.

Figure 3 qualitatively demonstrates the spatial distribution provided by the gel dosimeter, showing an isosurface representation of the reconstructed optical CT image, with contours selected at 64% and 83% of d_{max}. When using this technique to analyse a radiation field one would select contours at whichever level is required for purpose. Acquisition of optical CT data in slices occupied by the scintillator is corrupted as the scintillator and masking sheath is optically opaque and thus leads to artefacts arising from the undersampling of projections through these slices. Therefore slices corresponding to the scintillator and those immediately surrounding have been removed from figure 3. The data loss is an artefact only and in practical use the scintillator is recommended to be placed away from key locations in the radiation field to ensure no loss of critical spatial data.

Figure 4 shows the temporal radiation dose measurement at the location of the scintillator. The temporal scintillator data clearly shows the presence of two beams at different times, intensities, and duration. Because the scintillator has been pre-calibrated, the measured data will also indicate any errors in the output of the linear accelerator, both in radiation dose rate or exposure time. This would not otherwise be apparent in a 3D gel dosimeter measurement alone. Noise in the figure is due to quantum noise in the detector electronics as well as contributions from beam fluctuations at the time of sampling.

Ideally, the measurements of each detector should not be perturbed by the presence of the other. For example, if the scintillator was of a significantly different density, the radiation dose received by the gel dosimeter would show a 'shadow' of the scintillator in critical 'downstream' regions. Figure 5 shows comparative plots of the optical density of the gel dosimeter along the direction of the radiation beam, with error bars representing the standard deviation of the surrounding 3 mm × 3 mm region. Represented in the figure are depth dose data along the central axis of the beam which passes through the centre of the scintillator, and off axis data located within the radiation field in the gel dosimeter but not passing through the scintillator. The figure clearly shows the expected depth-dose curve as the beam transits the gel dosimeter in both sets of data located within the radiation field with a loss of data in the slices corresponding to the location of the scintillator. There is a region of reduced gel response immediately surrounding the location of the scintillator. Oxygen contamination decreases the sensitivity of polymer gel dosimeters [14] and it is likely that the presence of the scintillator and sheath in the gel allowed diffusion of oxygen in the time between manufacture, irradiation and imaging, thus suppressing the response of the gel to radiation. Previous studies with acyrlamide based gels have shown that oxygen diffuses at a rate of 8 ($\pm$2) x 10^{-6} cm^1 s^{-1}.[32]. At regions of further depth the depth dose data for both in-field measurements match, thus showing negligible perturbation of dose further downstream by the scintillator. Therefore, these results suggest that this technique would be suitable for use providing the scintillator is placed further than 1cm from critical regions in the irradiation.

Discussion

The interpretation of the data from these measurements will naturally depend on the response characteristics of each of the detectors; good practice would therefore necessitate each detector to be fully characterised before use. For example, the PAGAT type gel dosimeter used here for the 3D spatial dose mapping has previously been shown to have an asymptotic relationship to total dose [16]; conversions of optical density data, shown in Figure 3, to dose must therefore account for this relationship. It should be noted however that in PAGAT gel dosimeters a linear relationship between optical density and dose is generally assumed up to 7 Gy [16]; the maximum dose used here was less than this amount and therefore a linear dose response has been approximated in this work.

In addition to providing quasi-4D dosimetry, this method enhances traditional gel dosimetry measurements by enabling a calibrated dose point to be acquired within the gel itself. Previously gel dosimeters have been restricted to either relative dose measurements or calibration via secondary methods such as separate vials or re-production of an identical gel in a second container, both methods of which may affect the response of the gel dosimeter through variations in chemical composition, temperature history [33-35] or dose inaccuracies resulting from varying scatter conditions in different container geometries [36, 37]. Furthermore, Taylor *et al* [36, 37] have shown that a single large container is the most dosimetrically accurate geometry for gel dosimetry; inclusion of both detectors in the same volume ensures the most accurate results. Therefore, the inclusion of a plastic scintillator in a large container provides the opportunity for absolute dose measurements with gel dosimetry. Future work is required to refine the technique used in this feasibility study, for example the reduction of oxygen contamination at the immediate surrounds of the scintillator requires attention.

The extraction of the dose information is not restricted to optical computed tomography, for example, it has been shown that there is minimal interference with MRI image quality with the presence of a scintillating fibre within a gel dosimeter [38, 39] The detectors that can be used in this technique are not restricted to those employed here, for example, an excellent candidate for the 3D spatial detector would be polyurethane PRESAGE dosimeters [17] which would alleviate the requirement to remove data close to the scintillator and walls due to oxygen contamination. Similarly, for the nuclear industry and other industrial uses, detectors such as the RadBall [40, 41]could

provide a suitable spatial detector, or in the case of very high dose rate materials such as plastics [42] have been shown to react to ionising radiation and would combine well with the temporal measurements of an organic plastic scintillator.

The existence of Cerenkov radiation in the scintillator and optical fibre will cause an additional component to the signal. Several authors have discussed approaches to reduce interference of Cerenkov radiation in plastic scintillator measurements [43-46]. In our case the effects of Cerenkov radiation within the scintillator and optical fibre was minimized due to a 90 degrees irradiation angle and selection of components spectrally incompatible with Cerenkov light; however it is likely that the measured signal does contain a component of Cerenkov radiation. Because the same volume of optical coupling fibre (and full volume of the scintillator) was irradiated in both the calibration and the container irradiation, the same proportion of Cerenkov radiation occurred on both occasions and thus the calibration is adequate for this equivalent geometry and beam energy. Therefore, for the technique described in this work to be reliable it requires that the same volume of scintillator and optical fibre be irradiated at calibration and use. For applications where a different amount of the optical coupling fibre is irradiated by each beam (for example IMRT), an alternative Cerenkov rejection approach should be used [46-48].

Conclusion

In this work we have shown that the combination of two radiation detectors, one providing a 3D spatial mapping of dose and one providing temporal variation in dose rate, can be used to produce a 4D-hybrid radiation detection system. Typically, a gel dosimeter only provides dose information integrated over time, thus temporal information is lost. This work shows that the novel addition of temporal information to integrating 3D spatial dosimetry has been demonstrated to be feasible. This technique will provide a valuable means to fully characterize ionizing radiation fields.

References

1. R.J. Schulz and A.R. Kagan, *On the role of intensity-modulated radiation therapy in radiation oncology.* Med. Phys., 2002. **29**(7): p. 1473-1482.

2. M. Descovich, B. Fowble, A. Bevan, N. Shchechter, c. Park and P. Xia, *Comparison between hybrid direct aperture optimized intensity modulated radiotherapy and forward planning intensity modulated radiotherapy for whole breast irradiation.* Int. J. Radiat. Oncol. Biol. Phys., 2010. **76**: p. 91-99.

3. P.M. Evans, E.M. Donovan, M. Partridge, P.J. Childs, D.N. Convery, B.L. Suter and J.R. Yarnold, *The delivery of intensity modulated radiotherapy to breast using multiple static fields.* Raiother. Oncol., 2000. **57**: p. 79-89.

4. T. Bortfield, *IMRT: a review and preview.* Phys. Med. Biol., 2006. **51**: p. R363-R379.

5. S. Dieterich, K. Cleary, W. D'Souza, M. Murphy, K.H. Wonh and P. Keall, *Locating and targeting moving tumors with radiation beams.* Med. Phys., 2008. **35**(12): p. 5684-5694.

6. H. Fricke and S. Morse, *The chemical action of roentgen rays on dilute ferrous sulfate solutions as a measure of radiation dose.* Am. J. Roentgenol. Radium Therapy Nucl. Med., 1927. **18**: p. 430-432.

7. J.C. Gore, Y.S. Kang and R.J. Schulz, *Measurement of radiation dose distributions by nuclear magnetic resonance (NMR) imaging.* Phys. Med. Biol., 1984. **29**: p. 1189-1197.

8. J.C. Gore, Y.S. Kang and R.J. Schulz, *Dose-response curves for Fricke-infused agarose gels as obtained by nuclear magnetic resonance.* Phys. Med. Biol., 1990. **34**: p. 1611-1622.

9. C. Baldock, Y. De Deene, S.J. Doran, G.S. Ibbott, A. Jirasek, M. Lepage, K.B. McAuley, M. Oldham and L.J. Schreiner, *Polymer Gel Dosimetry.* Phys. Med. Biol., 2010. **55**(5): p. R1-63.

10. M.J. Day and G. Stein, *Chemical effects of ionizing radiation in some gels.* Nature, 1950. **166**: p. 1146-1147.

11. R.B. Mesrobian, P. Ander, D.S. Ballantine and G.J. Dienes, *Gamma-ray polymerization of acrylamide in the solid state.* J. Chem. Phys., 1954. **22**: p. 565-566.

12. H.L. Andrews, R.E. Murphy and E.J. LeBrun, *Gel dosimeter for depth dose measurements.* Rev. Sci. Inst., 1957. **28**: p. 329-332.

13. M.J. Maryanski, J.C. Gore, R.P. Kennan and R.J. Schulz, *NMR relaxation enhancement in gels polymerized and cross-linked by ionizing radiation: A new approach to 3D dosimetry by MRI.* Magn. Reson. Imaging, 1993. **11**: p. 253-258.

14. M.J. Maryanski, R.J. Schulz, G.S. Ibbott, J.C. Gatenby, J. Xie, D. Horton and J.C. Gore, *Magnetic resonance imaging of radiation dose distributions using a Polymer-gel Dosimeter.* Phys. Med. Biol., 1994. **39**: p. 1437-1455.

15. P.M. Fong, D.C. Keil, M.D. Does and J.C. Gore, *Polymer gels for magnetic resonance imaging of radiation dose distributions at normal room atmosphere.* Phys. Med. Biol., 2001. **46**: p. 3105-3113.

16. A. Venning, B. Hill, S. Brindha, B.J. Healy and C. Baldock, *Investigation of PAGAT polymer gel dosimeter using magnetic resonance imaging.* Phys. Med. Biol, 2005. **50**: p. 3875-3888.

17. J.A. Adamovics and M.J. Maryanski, *Characterisation of PRESAGE (TM): A new 3-D radiochromic solid polymer dosemeter for ionising radiation.* Radiation Protection Dosimetry, 2006. **120**: p. 107-112.

18. T. Gorjiara, R. Hill, Z. Kuncic, J.A. Adamovics, S. Bosi, J. Kim and C. Baldock, *Investigation of radiological properties and water equivalency of PRESAGE® dosimeters* Med. Phys., 2011. **38**(4): p. 2265-2274.

19.　　N.A. Baily, R.A. Horn and T.D. Kampp, *Flouroscopic visualization of megavoltage therapeutic X-ray beams.* Int. J. Radiat. Oncol. Biol. Phys., 1980. **6**: p. 935-939.

20.　　H. Meertens, M. van Herk and J. Weeds, *A liquid ionization detector for digital radiography of therapeutic megavoltage photon beams.* Phys. Med. Biol., 1984. **30**: p. 313-321.

21.　　W. van Etmpt, L. McDermott, S. Nijsten, M. Wendling, P. Lambin and B. Mijnheer, *A literature review of electronic portal imaging for radiotherapy dosimetry.* Radiotherapy and Oncology, 2008. **88**(3): p. 289-309.

22.　　P.A. Jursinic and B.E. Nelms, *A 2-D diode array and analysis software for verification of intensity modulated radiation therapy delivery.* Med. Phys., 2003. **30**(5): p. 870-879.

23.　　V. Feygelman, D. Opp, K. Javedan, A.J. Saini and G. Zhang, *Evaluation of a 3D diode array dosimeter for heclical tomotherapy delivery QA.* Med. Dosim., 2010. **35**(4): p. 324-329.

24.　　G.H. Yan, B. Lu, J. Kozelka, C. Liu and J.G. Li, *Calibration of a novel four-dimensional diode array.* Med. Phys., 2010. **37**(1): p. 108-115.

25.　　W. van Elmpt, L. McDermott, S. Nijsten, M. Wendling, P. Lambin and B. Mijnheer, *A literature review of electronic portal imaging for radiotherapy dosimetry.* Radiotherapy and Oncology, 2008. **88**(3): p. 289-309.

26.　　SaintGobain, *Scintillation products.* 2008, Saint Gobain Ceramics & Plastics.

27.　　J.V. Trapp, T. Kairn, S. Crowe and A. Fielding, *Internal calibration of gel dosimeters: A feasibility study.* Journal of Physics: Conference Series, 2009. **164**(012014): p. 1-5.

28.　　K. Williams, N. Robinson, J.V. Trapp, T. Ackerly, R. Das, P. Kemp and M. Geso, *A portable organic plastic scintillator dosimetry system for low energy X-rays: A feasibility study using an Intraoperative X-ray unit as the radiation source.* Journal of Medical Physics, 2007. **32**(2): p. 73-76.

29.　　S. Khoei, J.B. Moorrees, C.M. Langton and J. Trapp, *An investigation of the pre-irradiation temporal stability of PAGAT gel dosimeters.* Journal of Physics: Conference Series, 2010. **250**: p. 012019.

30.　　Y. De Deene, K. Vergote, C. Claeys and C. De Wagter, *The fundamental radiation properties of normoxic polymer gel dosimeters: a comparision between a methacrylic acid based gel and acrylamide based gels.* Phys. Med. Biol., 2006. **51**: p. 653-673.

31.　　A. Karlsson, H. Gustavsson, S. Mansson, K.B. McAuley and S.A.J. Back, *Dose integration characteristics in normoxic polymer gel dosimetry investigated using sequential beam irradiation.* Phys. Med. Biol., 2007. **52**: p. 4697-4706.

32.　　S. Hepworth, M.O. Leach and S.J. Doran, *Dynamics of Polymerization in Polyacrylamide Gel (PAG) Dosimeters: (II) Modelling Oxygen Diffusion.* Phys. Med. Biol., 1999. **44**: p. 1875-1884.

33.　　Y. De Deene, P. Hanselaer, C. De Wagter, E. Achten and W. De Neve, *An investigation of the chemical stability of a monomer/polymer gel dosimeter.* Phys. Med. Biol., 2000. **45**: p. 859-878.

34.　　E. Dumas, G. Leclerc and M. Lepage, *Effect of container size on the accuracy of polymer gel dosimetry.* Journal of Physics: Conference Series, 2006. **56**: p. 239-241.

35.　　Y. De Deene, G. Pittomvils and S. Visalatchi, *The influence of cooling rate on the accuracy of normoxic polymer gel dosimeters.* Phys. Med. Biol., 2007. **52**: p. 2719-2728.

36.　　M.L. Taylor, R. Franich, P.N. Johnston, M. Miller and J.V. Trapp, *Systematic variations in polymer gel dosimeter calibration due to container influence and deviations from water equivalence.* Phys. Med. Biol., 2007. **52**: p. 3991-4005.

37.　　M.L. Taylor, R. Franich, J.V. Trapp and P.N. Johnston, *A comparative study of the effect of calibration conditions on the water equivalence of a range of gel dosimeters.* IEEE Transactions on Nuclear Science, 2009. **56**(2): p. 429-436.

38.　　L. Archambault, G. Leclerc, L. Beaulieu and M. Lepage, *Absolute calibration of polymer gel dosimeter using scintillating fibres.* J. Phys. Conf. Ser., 2006. **56**: p. 242-244.

39.   N.M. Tremblay, V. Hubert-Tremblay, R. Bujold, L. Beaulieu and M. Lepage, *Improvement in the accuracy of polymer gel dosimeters using scintillating fibres.* Journal of Physics: Conference Series, 2010. **250**: p. 10.1088.

40.   S.J. Doran, S.J. Stanley, P.M. Jenneson, E. Prott and J.A. Adamovics, *RadBall: A new departure for 3D dosimetry.* J. Phys. Conf. Ser., 2009. **164**: p. 012042.

41.   E.B. Farfan, T.Q. Foley, G.T. Jannik, L.J. Harpring, J.R. Gordon, R. Blessing, J.R. Coleman, C.J. Holmes, M. Oldham, J.A. Adamovics, and S.J. Stanley, *RadBall technology testing in the Savannah River site's Health Physics Instrument Calibration Laboratory.* Journal of Physics: Conference Series, 2010. **250**: p. 10.1088/1742-6596/250/1/012080.

42.   J.W. Boag, G.W. Dolphin and J. Rotblat, *Radiation dosimetry by transparent plastics.* Radiation Research, 1958. **9**: p. 589-610.

43.   A.S. Beddar, T.R. Mackie and F.H. Attix, *Water-equivalent plastic scintillation detectors for high-energy beam dosimetry: I. Physical characteristics and theoretical considerations.* Phys. Med. Biol., 1992. **37**(10): p. 1883-1900.

44.   S.F. deBoer, A.S. Beddar and J.A. Rawlinson, *Optical filtering and spectral measurements of radiation induced light in plastic scintillation dosimetry.* Phys. Med. Biol., 1993. **38**: p. 945-958.

45.   J.M. Fontbonne, G. Iltis, G. Ban, A. Battala, J.C. Vernhes, J. Tillier, N. Bellaize, B. Tamain, K. Mercier and J.C. Motin, *Scintillating fibre dosimeter for radiation therapy accelerator.* IEEE Trans. Nucl. Sci., 2002. **49**: p. 2223-2227.

46.   J. Lambert, Y. Yin, D.R. McKenzie, S. Law and N. Suchowerska, *Cerenkov-free scintillation dosimetry in external beam radiotherapy with an air core light guide.* Phys. Med. Biol., 2008. **53**: p. 3071-3080.

47.   L. Archambault, T.M. Briere, F. Ponisch, L. Beaulieu, D.A. Kuban, A. Lee and S. Beddar, *Toward a real-time in vivo dosimetry system using plastic scintillation detectors.* Int. J. Radiation. Onc. Biol. Phys., 2010. **78**(1): p. 280-287.

48.   A.S. Beddar, S. Law, N. Suchowerska and T.R. Mackie, *Plastic scintillation dosimetry: optimization of light collection efficiency.* Phys. Med. Biol., 2003. **48**: p. 1141-1152.

Figure 1.   The scintillator/gel dosimeter immediately after irradiation. Two beams of different intensities were used and neither the container nor linear accelerator were moved between beams, therefore both beams irradiated the system in identical geometry. The optical changes to the gel dosimeter resulting from the radiation dose can be seen along the central axis of the container.

Figure 2.   Data for the calibration of the organic plastic scintillator. The scintillator system outputs a signal whose frequency varies with dose. A linear response is noted for the range of dose rates covered in this work.

Figure 3.   Typical 3D isosurfaces acquired from the post irradiation optical CT image of the gel dosimeter as located in the container (blue). Because the optical density is proportional to radiation dose, the isosurface can be converted to a dose contour. In this case the green surface represents 64% of the maximum dose and the (darker) red represents 83% of the maximum dose.

Figure 4.   Temporal organic plastic scintillator measurement during the irradiation of the container. Although the same dose was delivered with each beam, the dose rate and time was varied.

Figure 5.   Changes in the gel dosimeter optical density along the axis of the cylinder. The upper panel shows the optical CT data for two sets of in-field data: one intersecting the scintillator and the other within the radiation field but not intersecting the scintillator. The bottom panel shows the difference between the two data sets.

Table 1 – Composistion of 1 kg of PAGAT gel dosimeter

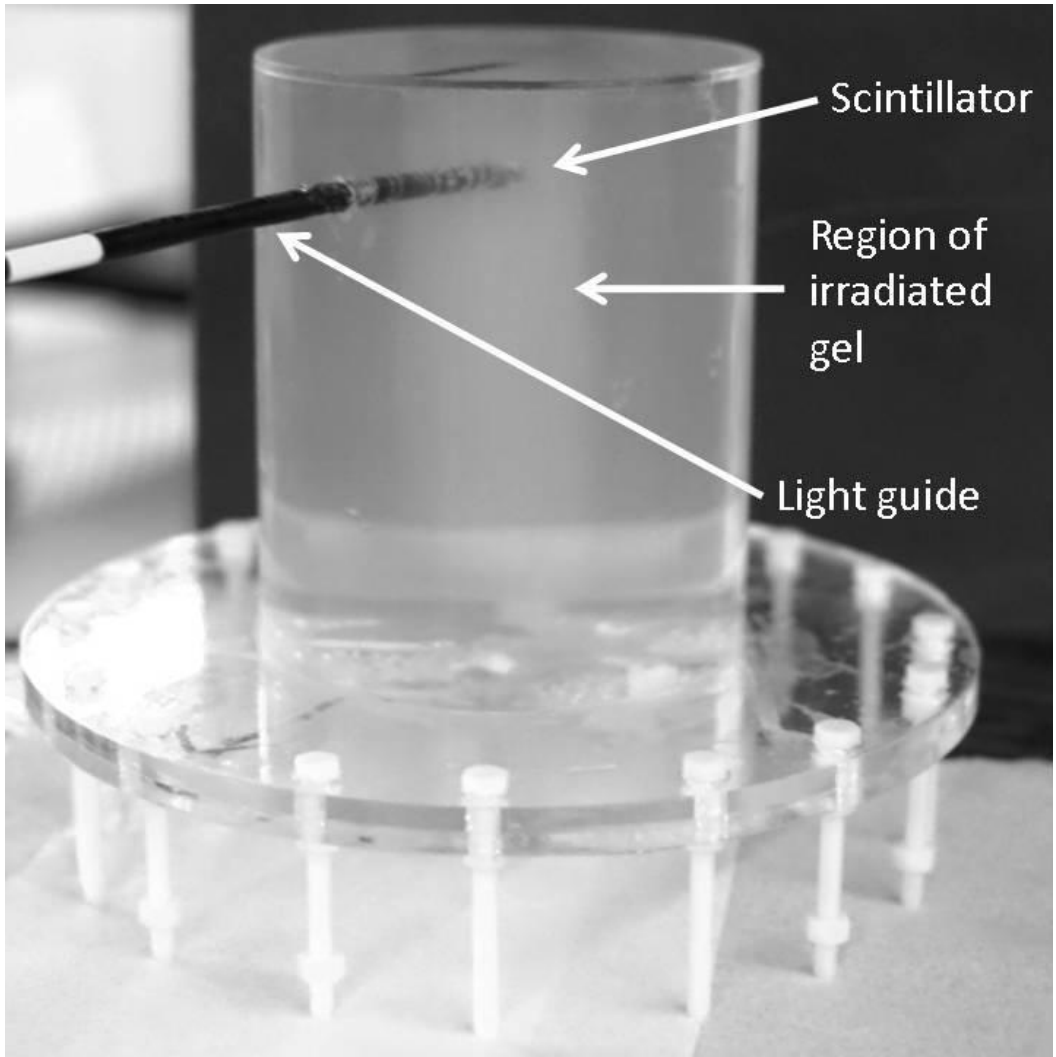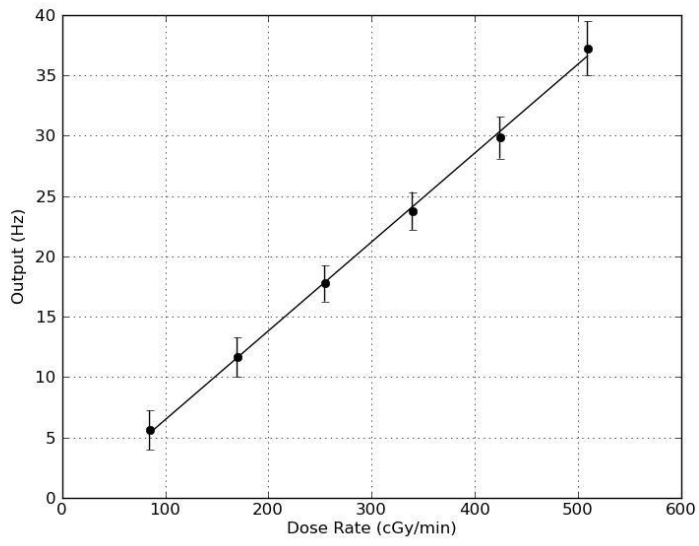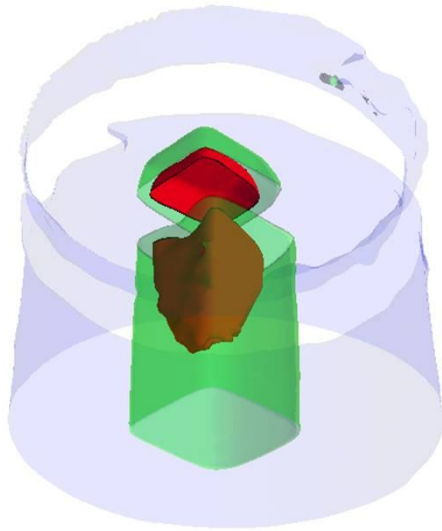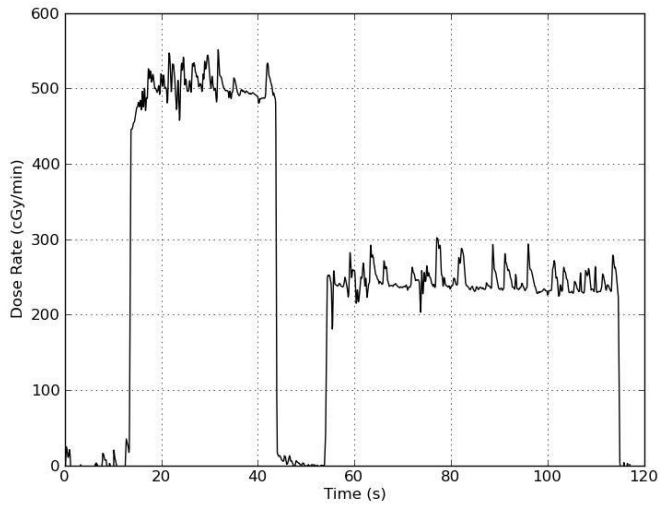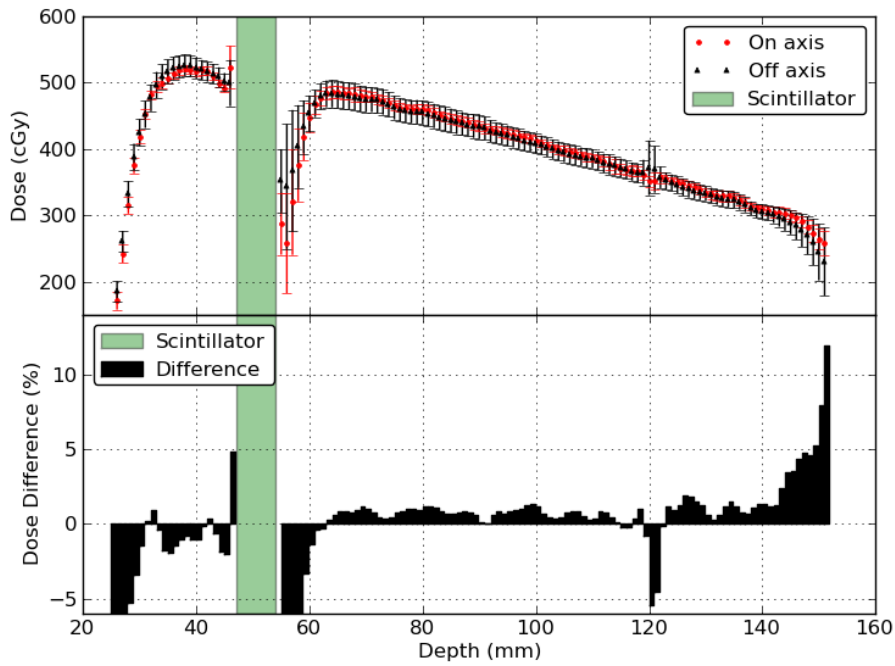| Component |
| --- |
| Water 859.5 g |
| Gelatin 300 Bloom Type A 50 g |
| N,N' Methylene bis acrylamide 45 g |
| Acrylamide 45 g |
| Hydroquinone 0.001 g |
| Tetrakis Hydroxy Phosphonium Chloride 1.0 g |

Figure 1

Figure 2

Figure 3

Figure 4

Figure 5